Supplement of The Cryosphere, 18, 1467–1493, 2024
https://doi.org/10.5194/tc-18-1467-2024-supplement

The Cryosphere
Open Access

Supplement of

Subglacial valleys preserved in the highlands of south and east Greenland record restricted ice extent during past warmer climates

Guy J. G. Paxman et al.

Correspondence to: Guy J. G. Paxman (guy.j.paxman@durham.ac.uk)

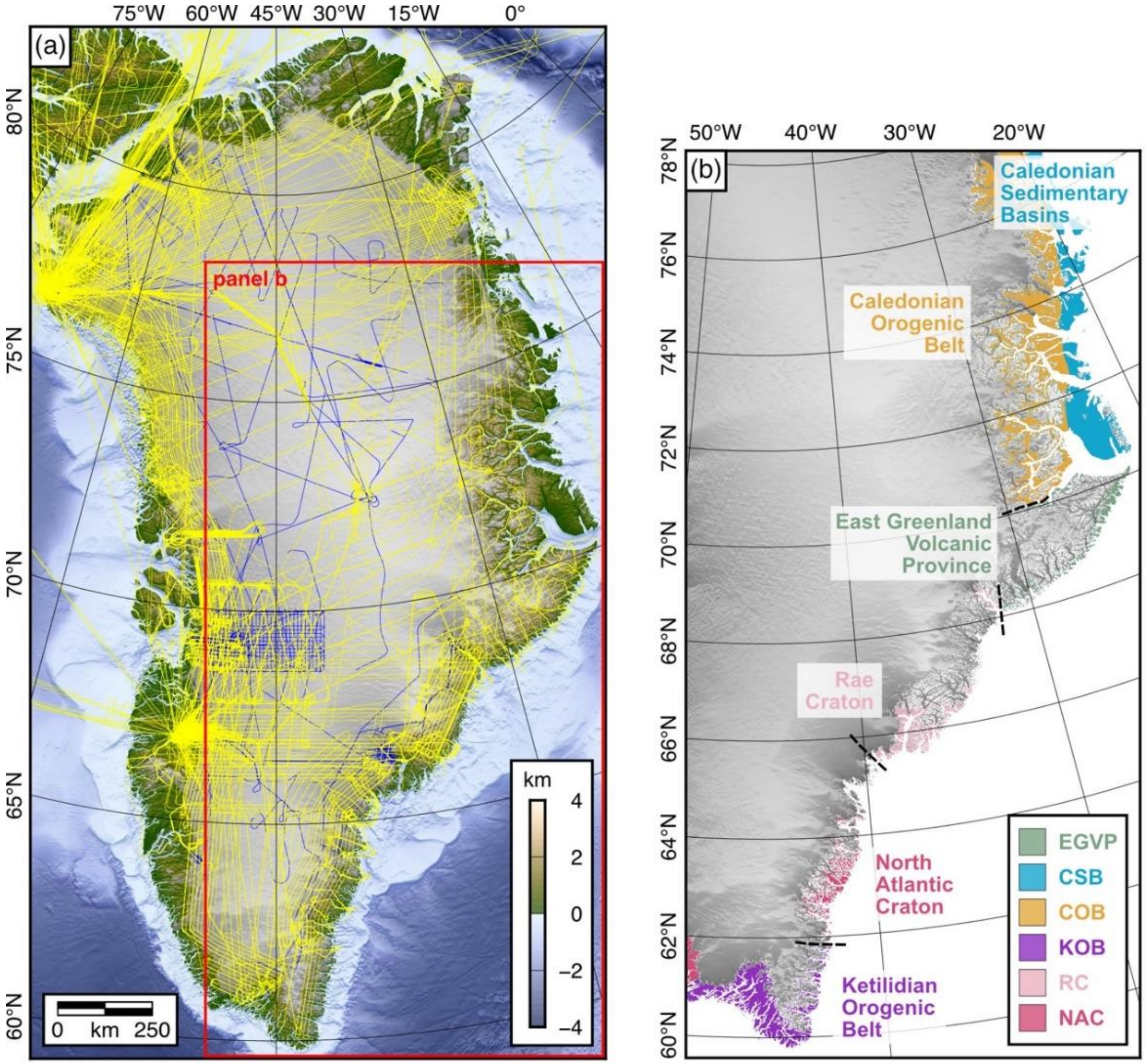

Figure S1: Radio-echo sounding coverage and major geological provinces of Greenland. (a) Radio-echo sounding survey lines from Operation IceBridge (yellow; 2010–2019) and Center for Remote Sensing and Integrated Systems (blue; pre-2010) (Paden et al., 2019). These lines were used to map subglacial valley cross-profiles (Paxman, 2023). The Greenland Ice Sheet surface is shaded in grey (Howat et al., 2022); land surface topography and seafloor bathymetry are displayed according to the colour scale (relative to mean sea level) (Morlighem et al., 2017). (b) Major geological provinces exposed along the eastern margin of Greenland (Henriksen et al., 2009). Provinces are listed in stratigraphic order in the legend. Dashed black lines indicate the approximate locations of boundaries between provinces.

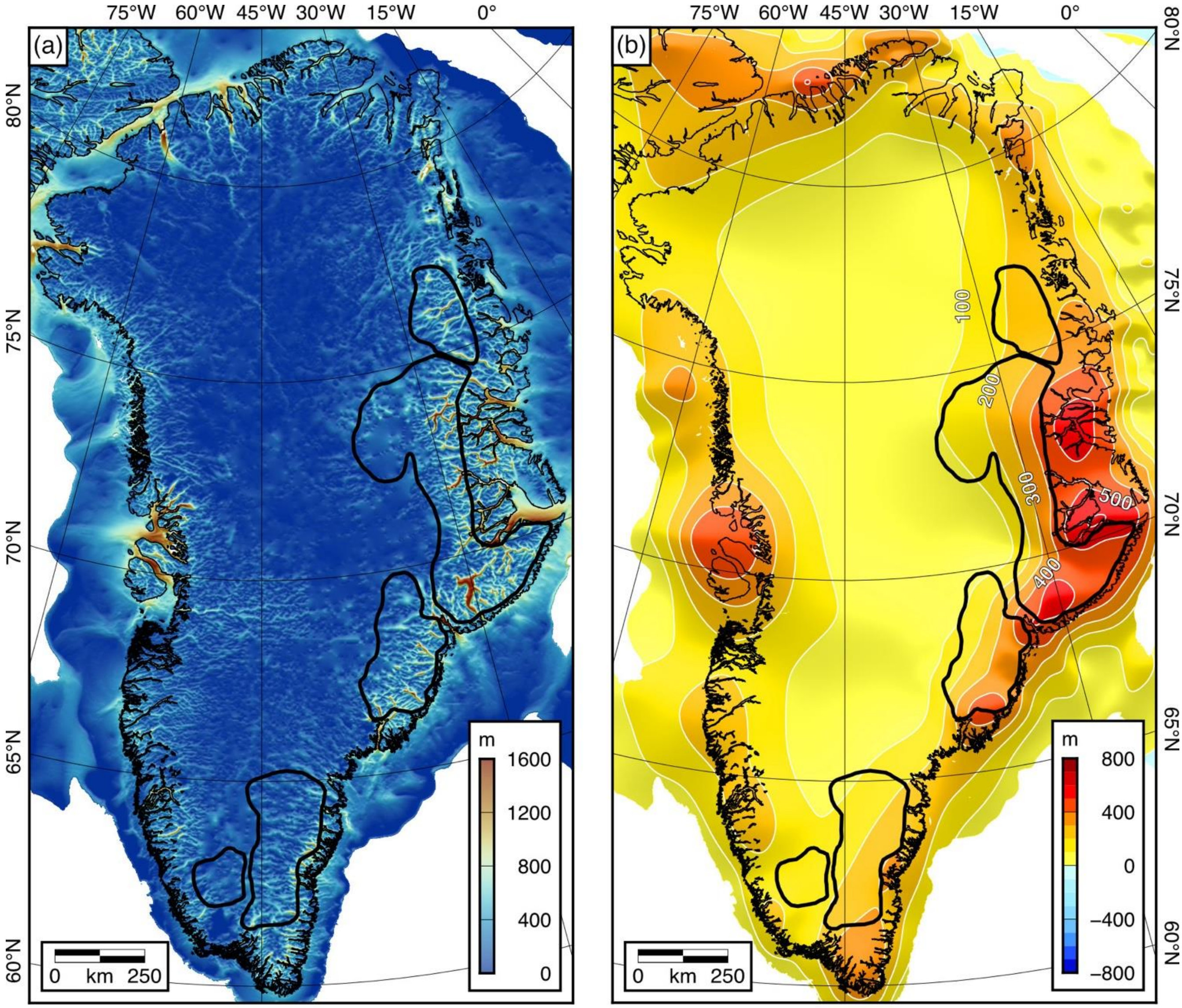

Figure S2: Flexural isostatic response to glacial valley, fjord, and trough incision. (a) Estimated distribution of incised thickness across Greenland and the adjacent continental shelf. The thickness of erosion was estimated by interpolating a smooth accordant surface between topographic 'highs' (i.e., peaks and plateaux) and differencing the ice-free BedMachine v.5 digital elevation model (Morlighem et al., 2020; Paxman et al., 2022) from this surface (for more details the reader is referred to Medvedev et al. (2013) and Pedersen et al. (2019)). Black polygons mark the extent of the mapped palaeo-glacial valley network. (b) Flexural uplift resulting from the unloading of the eroded material shown in panel a. The flexure was computed using an elastic plate model with a spatially variable effective elastic thickness (Paxman et al., 2021; Steffen et al., 2018). Contour interval is 100 metres. To construct the bed topography used in our ice-sheet model experiments, this flexural response was subtracted from the ice-free BedMachine v.5 digital elevation model.

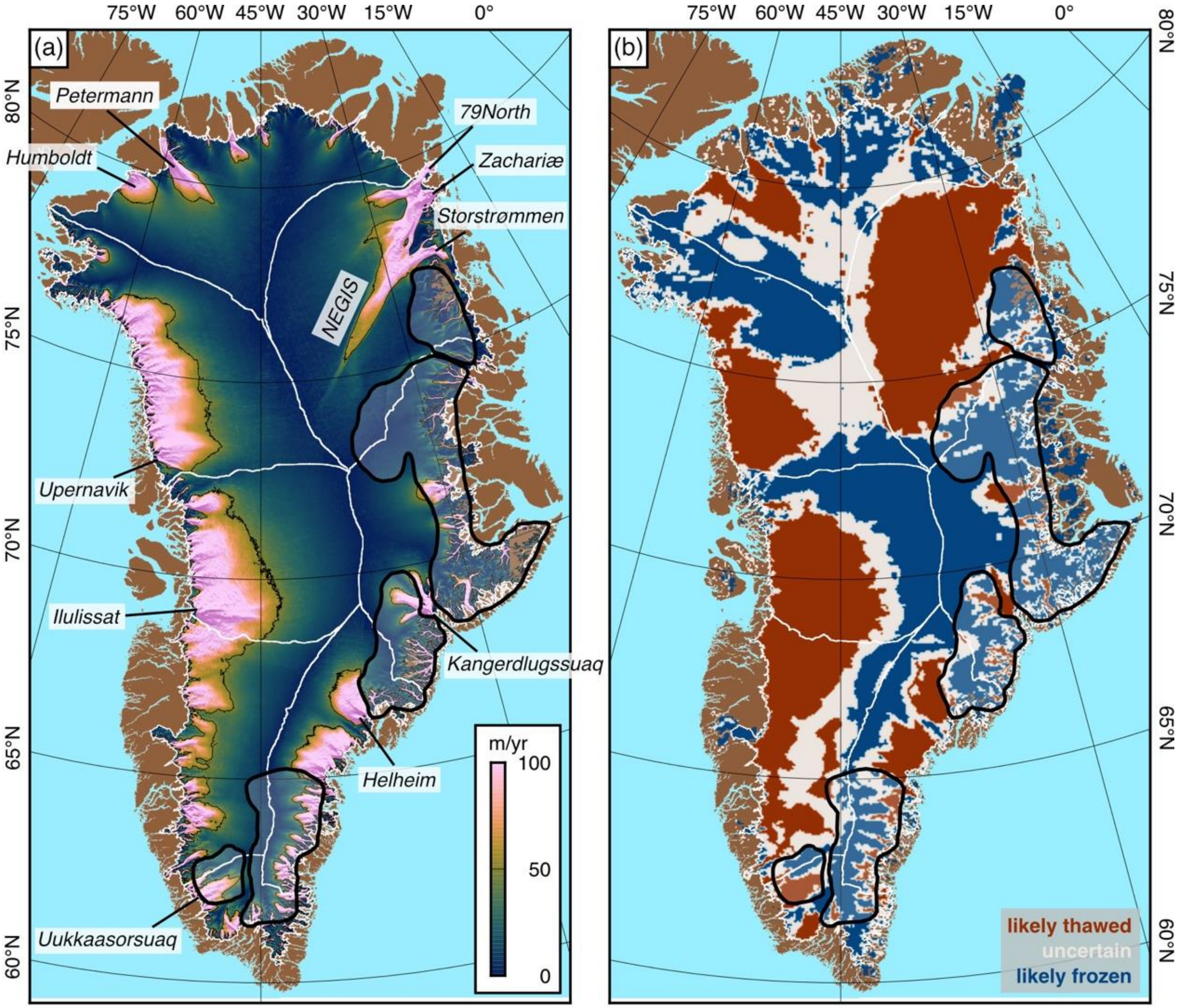

Figure S3: Contemporary Greenland Ice Sheet dynamics. (a) Ice surface velocity (Joughin et al., 2018). The 50 m/yr contour, an approximate threshold of the onset of fast flow, is marked by the thin black outline. Selected outlet glaciers are labelled. (b) Synthesis of the likely basal thermal state of the ice sheet (MacGregor et al., 2022). In both panels, thick black outlines denote the highland palaeo-glacial valley limits mapped in this study. White lines delineate major ice-sheet drainage catchments (Zwally et al., 2012).

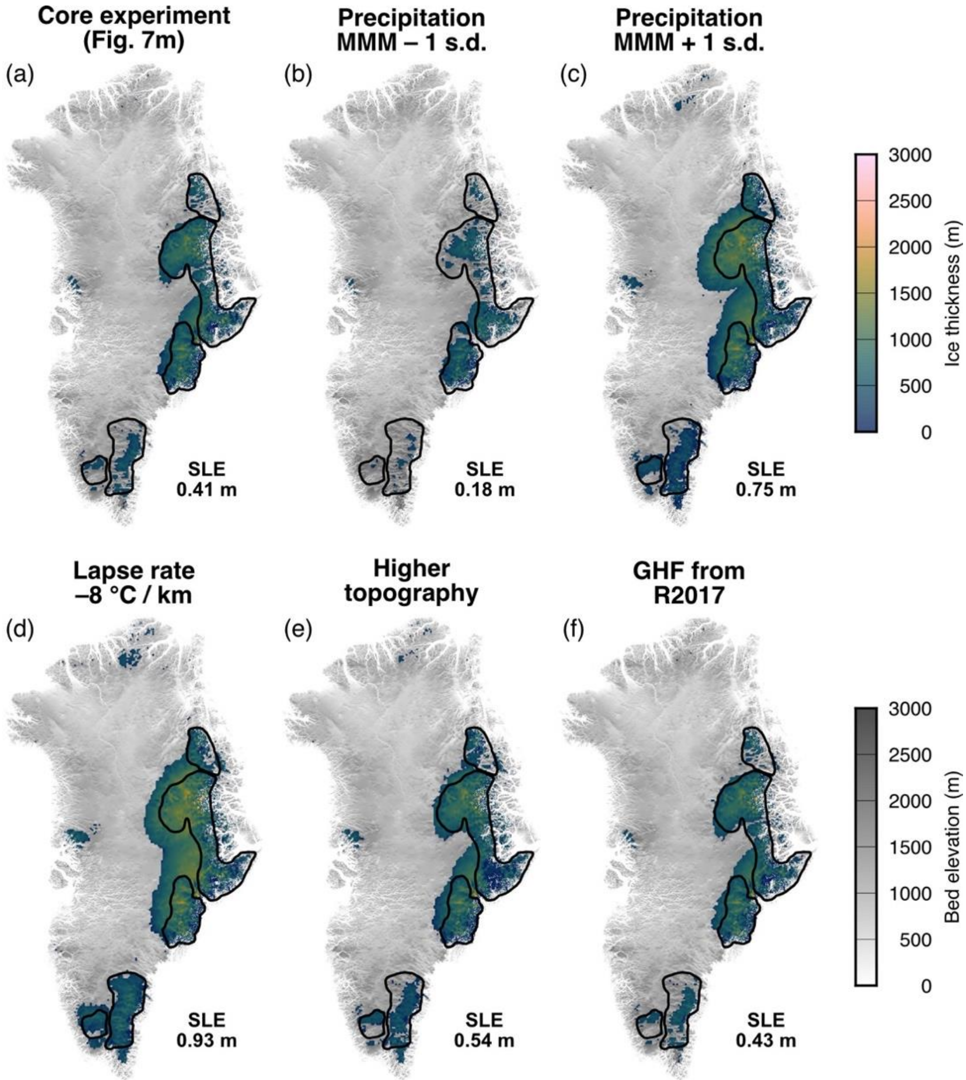

Figure S4: Sensitivity testing of modelled GrIS thickness to precipitation, atmospheric lapse rate, bed topography, and geothermal heat flux. (a) Control experiment with the temperature field that best-matches the mapped palaeo-glacial valley limit in the eastern highlands (panel m in Fig. 7 in the main manuscript). (b) Experiment with precipitation decreased to one standard deviation (s.d.) below the PlioMIP2 multi-model mean (MMM). (c) Experiment with precipitation increased to one standard deviation above the PlioMIP2 multi-model mean. (d) Atmospheric lapse rate increased to -8 °C km^{-1}. (e) Reconstructed pre-glacial bed topography increased to its maximum ('high') elevation scenario. (f) Geothermal heat flux (GHF) changed to the Rezvanbehbahani et al. (2017) (R2017) model. SLE = sea level equivalent.